Dipolar Intermolecular Interactions, Structural Development, and Electromechanical Properties in Ferroelectric Polymer Blends of Nylon-11 and Poly(vinylidene fluoride)

Qiong Gao and Jerry I. Scheinbeim*

Polymer Electroprocessing Laboratory, Department of Chemical and Biochemical Engineering, College of Engineering, Rutgers University, Piscataway, New Jersey 08854-0909

Received January 21, 2000; Revised Manuscript Received July 14, 2000

ABSTRACT: A new polymer blend was developed from two well-known ferroelectric polymers, nylon-11 and poly(vinylidene fluoride) (PVF_2), by mechanically mixing them in powder form. The intermolecular interactions between these two semicrystalline polymers was evidenced by the observed decrease of the glass transition temperature and melting points of nylon-11 with increasing PVF_2 concentration measured by temperature modulated differential scanning calorimetry (TMDSC). Fourier transform infrared spectroscopy (FTIR) was used to measure the shifts of several characteristic bands of nylon-11 and PVF_2 in the blends, which indicated specific interaction between the polar amide groups (CONH) in nylon-11 and the polar CF_2 groups in PVF_2. We observed that this interaction affected the crystallization behavior of both components in the blend. The nylon-11 hydrogen-bonded structure became more disordered as the PVF_2 concentration increased in the blend. PVF_2 developed a large proportion of polar crystal phases (I and III) in blends with high nylon-11 concentration instead of nonpolar phase II developed in pure PVF_2 under similar melt quench conditions. In the uniaxial drawing process, the phase transformation of PVF_2 from nonpolar phase II to the most polar phase I crystal form is more complete, and the resulting phase I crystals are more ordered than in pure PVF_2 as shown by FTIR and wide-angle X-ray diffraction (WAXD) studies. This structural change led to enhanced piezoelectric response and significantly improved high-temperature stability (up to160 °C) of piezoelectric properties in the blends, which enable this new polymeric material to be used in many new electroactive applications.

I. Introduction

Nylon-11 and PVF_2 are both intensively studied ferroelectric polymers.[1] PVF_2 has the highest piezoelectric response found so far in any polymer at room temperature.[2] Odd-numbered nylons have comparable ferroelectric response but low piezoelectric response at room temperature because the nylons have a higher glass transition temperature.[3] However, the nylons have better thermal stability resulting from the close-packed hydrogen-bonded sheet structure obtained after annealing.[15] This is a very attractive property since the thermal stability of the polarization of PVF_2 and other piezoelectric polymer materials is an important issue preventing their use in many unique applications. The motivation of the current study is to find the best possible combination of desirable properties of these two polymers.

The polar amide (CONH) groups in nylon-11 and the polar CF_2 group in PVF_2 along with their polar crystal structures enabled both polymers to be ferroelectric. In powder blends of these two polymers, strong intermolecular interactions might be expected from dipolar interactions between polar groups. It is well-known that the smaller the dipole moment difference, the more compatible the polymers,[4] such as in PVF_2 and poly(acrylic ester).[5] PVF_2 has been found actually miscible with many polymers with ester, ether, or carbonyl functional group in either main chain or side chain,[6] such as poly(vinyl methyl ketone) (PVMK), poly(tetramethylene adipate) (PTMA), poly(vinyl acetate) (PVAc), and poly(*N*-methylethylenimine) (miscible for volume fractions of PVF_2 larger than 50%), poly(*N*,*N*-dimethylacrylamide), poly(*N*-vinyl-2-pyrrolidone), and polyacrylates, e.g., poly(methyl methacrylate) (PMMA) and poly(ethyl methacrylate) (PEMA).[7] PVF_2 and amide-containing compounds having favorable interactions have been also observed in several blends such as nylon-6/PVF_2 blends[8] and PVF_2/ϵ-caprolactan blends.[9] Some amide-containing small organic molecules, e.g., *N*,*N*-dimethylacetamide (DMA) and *N*,*N*-dimethylformamide (DMF), are good solvents for PVF_2, although PVF_2 is essentially insoluble in most organic solvents. This type of interaction was also shown in nylon- and chlorine-containing polymer blends, such as in nylon-11/polyepichlorohydrin (PECH)[11] and poly(ϵ-caprolactone)/poly(vinyl chloride).[11] Nuclear magnetic resonance (NMR), differential scanning calorimetry (DSC), and transmission electron microscopy (TEM) showed that blending changed the motional states and crystal structures of the two components, even though each has large domain sizes in the solid state of the mechanically mixed blends. The motional freedom of the PECH chains decreased as the concentration of nylon-11 increased. The amorphous phase of nylon-11 changed little after blending, but increasing the PECH content of the blend caused the crystalline phase of nylon-11 to become disordered and the crystallinity of nylon-11 decreased.

A simple and useful way to assess the compatibility of polymer pairs is to use the solubility parameter, δ. Hansen's solubility parameter was a practical extension of the Hildebrand parameter method applied to polar and hydrogen-bonding systems. It is applicable to our system of nylon-11 and PVF_2. The average value of the solubility parameter for PVF_2 was found to be 23.2 $MPa^{1/2}$.[12] For nylon-11, no direct measurement of δ was

* Corresponding author. Tel 732 445-3669; Fax 732 445-0654; E-mail jis@rci.rutgers.edu.

10.1021/ma000111i CCC: $19.00
Published on Web 09/14/2000

found, but instead, we found that the average δ value of nylon-12 was 21.5 $MPa^{1/2}$.[13] Since the chemical structures of these two polyamides are similar, their solubility parameters should also be close. Direct evidence of this is suggested by the fact that the polymer−liquid interaction parameter, χ, with water of these two polyamides were very close: 3.2 for nylon-11 and 3.4 for nylon-12 at 25 °C.[8] The δ of nylon-11 should be slightly higher than that of nylon-12 because the density of polar groups and hydrogen bonds in nylon-11 is slightly higher. Therefore, the solubility parameters of nylon-11 should be approximately 23 $MPa^{1/2}$, very close to that of PVF_2. The intermolecular interaction parameter χ, between two polymers is given by

$$\chi \sim \frac{V_i}{RT}(\delta_i - \delta_j)^2$$

where T is the absolute temperature, R is the gas constant, and V_i is the molar volume. Therefore, the χ value for nylon-11 and PVF_2 should be very small. It is well-known that the smaller the χ value, the larger the compatibility. This predicts that these two polymers are either compatible or partially compatible.

In this paper, we first present evidence for intermolecular interactions, most likely the dipolar interactions between nylon-11 and PVF_2 chains, which include infrared bands shifts in both nylon-11 and PVF_2, and observed decreases in the glass transition and melting temperature of nylon-11 with increasing PVF_2 concentration in the blends. The effect of these intermolecular interactions on crystal structure development in the melt-quench process and the crystal phase transformation during the drawing process of melt-quenched samples was then studied by FTIR and WAXD. These structure changes affect the electroactive properties of the blends. The piezoelectric properties of the blends and their thermal stability were investigated and discussed on the basis of the crystal structure changes in the blends.

II. Experiments

We used a low-temperature fine powder mixing method as previously described[14] to produce the powder blends. The blended powder was melt-pressed between aluminum foils for 3 min and then quenched into an ice−water bath. These samples are referred to as melt-quenched films. The melt-quenched films were cold drawn at room temperature to a 3:1 draw ratio. These samples are referred to as drawn samples.

A temperature-modulated DSC 2910 from TA instruments was used to measure the glass transition temperature, T_g, and melting point, T_m, of the blends. The powder mixtures were packed in aluminum pans. The samples weighted ~9 mg. The samples were first heated to 210 °C at 50 °C/min heating rate, kept at 210 °C for 10 min, and then cooled slowly to −50 °C at a modulation mode with an oscillation amplitude of 0.5 °C and period of 60 s at an underlying heating rate of 2 °C/min. The TA instruments Graphware software was used to locate the T_g (inflection point) and T_m (peak position).

The infrared spectra were taken with a Nicolet Magna-550 and analyzed using OMNIC 4.1 software. All of the spectra were taken with 1 cm^{-1} resolution and with 200 scans of the sample ratioed with 200 scans of the reference beam. Attenuated total reflection (ATR) mode was used for strong absorption bands where the spectrum was automatically corrected for the wavenumber dependence of absorption. Transmission mode was used for intermediate and weak absorption bands. The polarized spectra were taken with a gold wire grid polarizer placed between sample and IR source. To minimize the polarization effects of prism, grating, and dispersion elements, samples were placed with the draw (orientation) axis at 45° with respect to the beam slits. The polarizer was oriented at 45°and 135° with respect to the beam slits. The sample chamber was purged with dry nitrogen at all times. Samples were stored in a desiccator before measurements to minimize water effects. Two major effects are produced by the presence of water in nylon-11. One is that the OH stretching absorption of water overlaps with the NH stretching adsorption of nylon-11. The other is that the presence of water changes the nature and extent of hydrogen bonding in nylon-11.

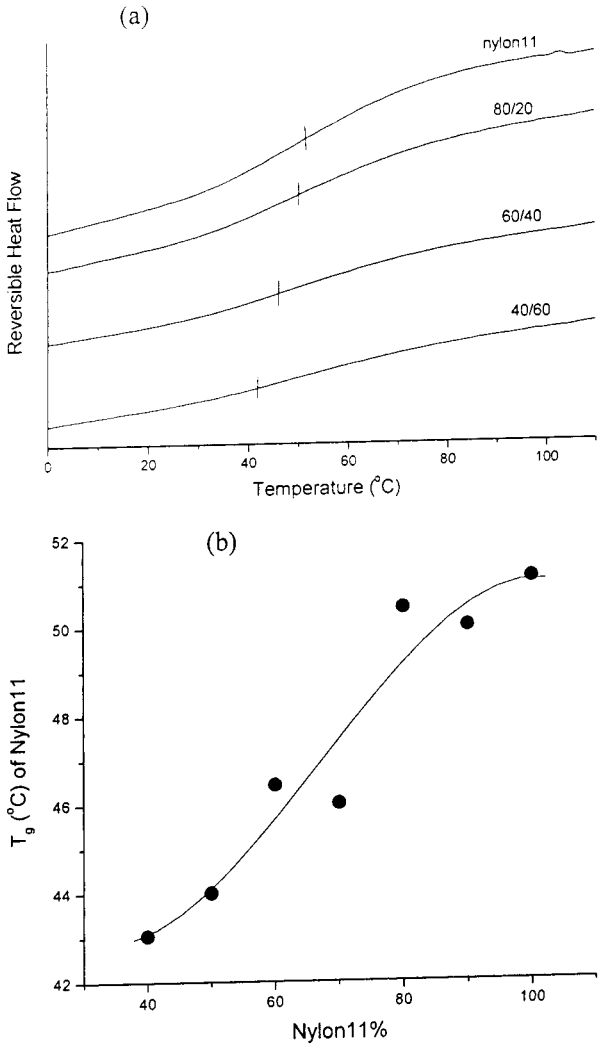

Figure 1. (a) DSC cooling traces (reversible heat flow) of nylon-11/PVF_2 blends with different compositions. (b) Composition dependence of nylon-11 glass transition temperatures T_g in nylon-11/PVF_2 blends.

For the poling, dielectric, and piezoelectric measurements, gold electrodes were deposited on opposing surfaces of the films by vacuum evaporation. Before the dielectric and piezoelectric measurements, the samples were poled at room temperature by application of a triangular-shaped electric field at a very low frequency of 1/640 Hz as described in a previous work.[14] A maximum poling field of 220 MV/m was used. The dielectric constant, ϵ, Young's modulus, C, and piezoelectric stress and strain coefficients, d_{31} and e_{31}, were measured at 104 Hz using a dynamic piezoelectric measurement apparatus described by Scheinbeim et al.[16]

III. Results and Discussion

1. Glass Transition and Melting Point of Nylon-11 in Blends. Figure 1a shows DSC cooling traces (reversible heat flow) of the powder blends with 2 °C/min cooling rate and ±0.5 °C/min modulation for pure

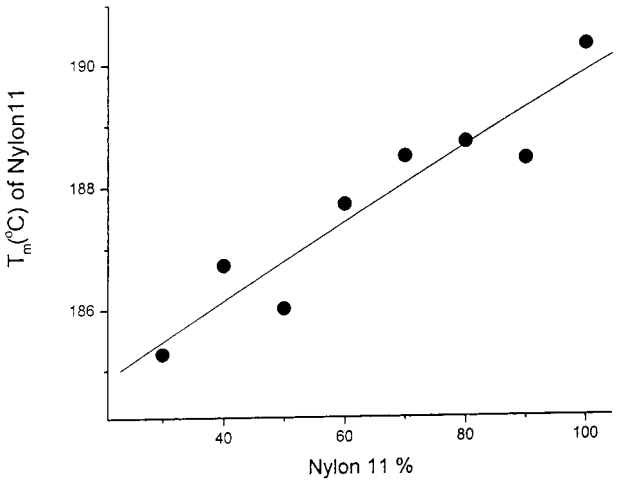

Figure 2. Composition dependence of the melting point of nylon-11 in nylon-11/PVF_2 blend.

nylon-11 and the blends with different compositions. The glass transition temperatures, determined from the inflection point of the reversible heat flow of the blends, are plotted as a function of the nylon-11 concentration and shown in Figure 1b. It is seen that, under the sample preparation conditions stated above, the blends exhibit a composition-dependent glass transition temperature which decreased from 51 to 41 °C as the nylon-11 concentration decreased from 100% to 40%. The change in T_g with composition we observed does not fit predictions of miscible blends since the T_g of PVF_2 is about −40 °C[16,17] and the T_g of nylon-11 is about 50 °C. However, we can say we observed a significant decrease of the T_g in nylon-11 with increased concentration of the lower T_g component, PVF_2, in the blends. This may indicate there is some level of intermolecular interactions in the amorphous regions of nylon-11/PVF_2 blends under our blend preparation conditions.

In semicrystalline polymer blends, the melting point change provides additional evidence for the intermolecular interaction in blends. Figure 2 shows that the melting point of nylon-11 decreased with decreasing nylon-11 concentration in the blend. It is known that in compatible blends the melting point of the crystalline component is usually lowered with respect to the pure polymer as a result of thermodynamically favorable interactions. The extent of the melting point depression in such systems could actually provide a measure of the interaction energy, the interaction parameter, χ, as described by a modified Flory−Huggins theory of polymer mixture.[12] But since we did not achieve equilibrium mixing, we do not attempt to estimate the interaction parameter here. However, this observed melting point depression of nylon-11 should be considered further evidence of interactions between nylon-11 and PVF_2 in this system of powder blends.

2. IR Band Shifts and Crystal Structure Development in Melt-Quenched Blends. IR spectroscopy can selectively measure molecular level interaction and localized chain conformation. In our case, most of the characteristic bands of nylon-11 and PVF_2 do not overlap. These include the N−H stretching at 3300 cm^{-1}, the CH_2 antisymmetric stretching υ_a at 2920 cm^{-1}, the CH_2 symmetric stretching υ_s at 2850 cm^{-1}, amide I at 1635 cm^{-1}, amide II at 1545 cm^{-1} in nylon-11, and 1180 cm^{-1} (CF_2 $(\upsilon_a)_i$), 1067 cm^{-1} (skeletal), 975 cm^{-1} (skeletal), 870 cm^{-1} (skeletal), 839 cm^{-1} (CH_2, $(rock)_i$ or skeletal), 532 cm^{-1} (CF_2, $(\delta)_o$), and 490 cm^{-1} (CF_2 $(twist)_i$) in PVF_2. Therefore, it is feasible to use FTIR to investigate any changes in the intermolecular interactions and chain conformations of nylon-11 and PVF_2 in the powder blends.

Figure 3a−e shows that the nylon-11 amide I, amide II, NH stretching, and CH_2 symmetric and antisymmetric stretching bands changed with blend composition. The amide I band of nylon-11 increased from 1635 to 1641 cm^{-1} as the nylon-11 concentration decreased from 100% to 3% as shown in Figures 3a. It also became broader as the nylon-11 concentration decreased as seen from the inset of Figure 3a. Figure 3b shows that the amide II band first decreased as the nylon-11 concentration decreased and then increased as the nylon-11 concentration decreased below ∼50%. The N−H stretching band of nylon-11 decreases from 3301 to 3294 cm^{-1} as its concentration decreased from 100% to 3% shown in Figure 3c. The decrease is slow and exhibits a change in curvature at ∼50% nylon after which a rapid decrease is observed as the nylon-11 concentration goes to zero. Parts d and e of Figure 3 show that the CH_2 symmetric and antisymmetric stretching bands increased from 2919 to 2923 cm^{-1} and from 2850 to 2851 cm^{-1}, respectively. All the above bands became broader as the nylon-11 concentration decreased in the blends. From these IR band changes, we may obtain a picture of the interactions at the interface between nylon-11 and PVF_2 as shown in Figure 4. The intermolecular interactions between nylon-11 and PVF_2 should be dipolar interaction between the functional amide group of CONH in nylon-11 and the CF_2 group in PVF_2. This model is based on the fact that we observed significant changes in the amide I and II and the N−H stretching bands of nylon-11 compared to the much smaller changes in the CH_2 symmetric and antisymmetric stretching bands.

The N−H stretching band shift to lower wavenumbers means the interaction between the N−H and C−F is stronger than the N−H and C═O interaction and implies that some hydrogen bonds between N−H and C═O are broken. The extent of intermolecular hydrogen bonding in nylon-11 may be decreased by the competing intermolecular interaction between nylon-11 and PVF_2. Therefore, nylon-11 may become more disordered in the blends as more PVF_2 is added. This is actually what we observed, shown by the amide I band change. It is well-known that the infrared absorption in the amide I region (1620−1690 cm^{-1}), the stretching vibrations of the carbonyl groups, reveals information concerning the secondary structure of polyamides.[18,19] The absorption around 1635 cm^{-1} is associated with the β-sheet structure, where the bands close to 1653 and 1646 cm^{-1} are associated with the helical and random portions of the polyamide, respectively. In our case, the 1635 cm^{-1} band observed in pure nylon-11 indicated the well-known hydrogen-bonded β-sheet structure of nylon-11.[20] In powder blends, this band shifted to higher wavenumbers, close to 1646 cm^{-1}, which indicated that the random portion of nylon-11 increased as its concentration decreased in the blends.

The dipolar intermolecular interactions between the nylon-11 and PVF_2 may also affect PVF_2 chain conformation and should be then reflected in IR band changes as well. Figure 5 shows the IR spectra of PVF_2 in the blends over the 920−820 cm^{-1} region. We see that the skeletal band at 870 cm^{-1} and the CH_2 rocking band at

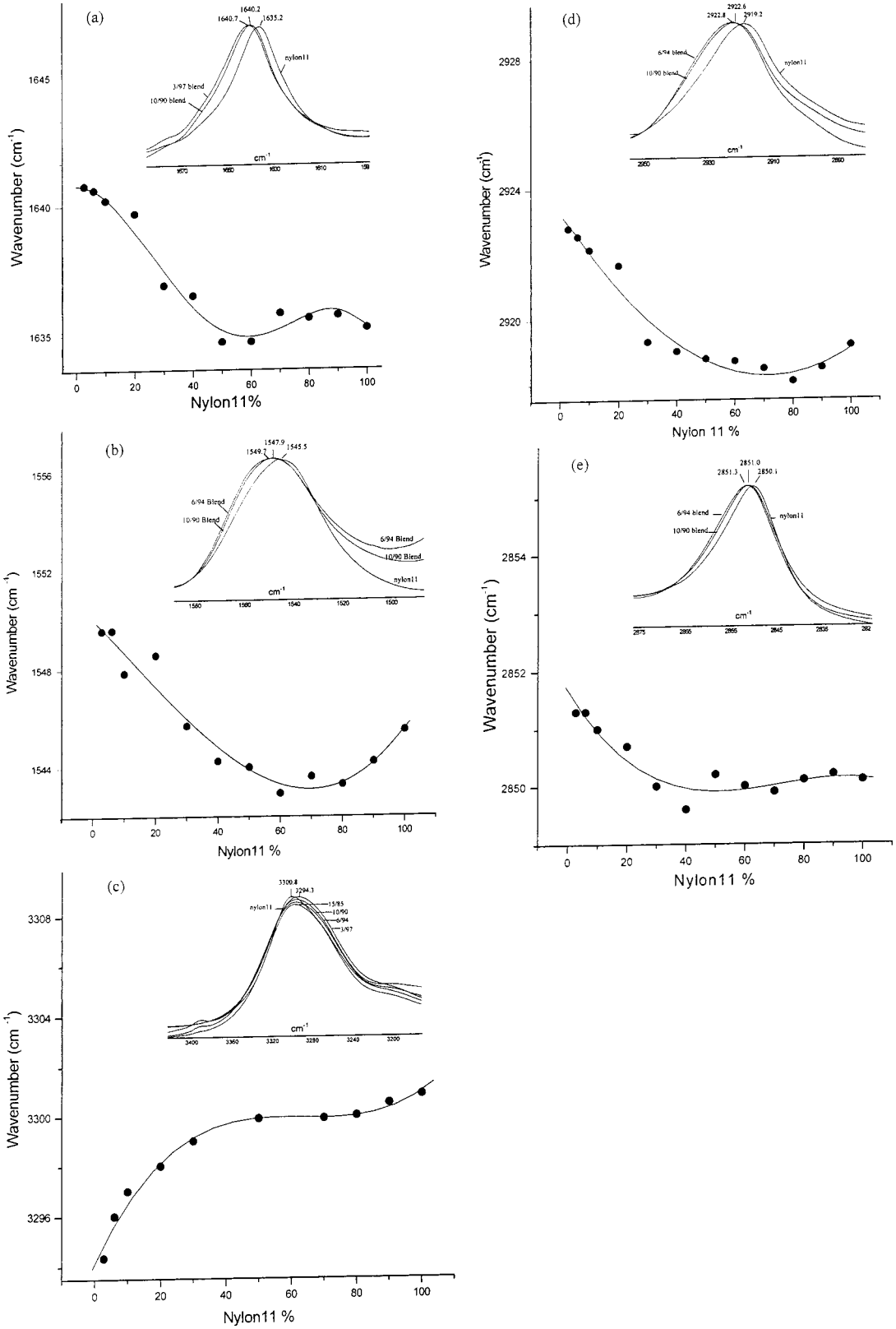

Figure 3. IR bands of nylon-11 change with its concentration in the blends: (a) amide I band, (b) amide II band, (c) N−H stretching band, (d) CH_2 antisymmetric stretching band, and (e) CH_2 symmetric stretching band.

840 cm^{-1} change with blend composition. The 880 cm^{-1} band decrease and became much broader as the nylon-11 concentration increased. The shape and position of the 840 cm^{-1} band also changed. Figure 6 shows the spectra of PVF_2 in blends over the 1100−440 cm^{-1} region after the subtraction of the nylon-11 absorbency. Besides the 870 and 840 cm^{-1} band shifts, the relative intensity of some bands in this region changed as well, such as the intensity of the 840, 510, and 440 cm^{-1} bands increased and the intensity of the 976, 854, 795, and 532 cm^{-1} bands decreased as nylon-11 concentration increased in the blends. This indicates that the crystal structure of PVF_2 changed with blend composition. It is known that PVF_2 can crystallize into several

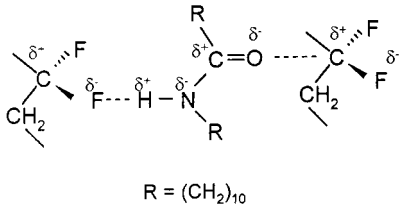

Figure 4. Schematic draw of the dipolar intermolecular interactions between nylon-11 and PVF_2.

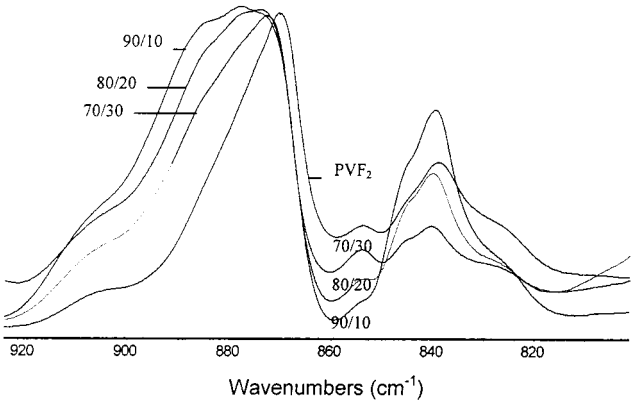

Figure 5. IR spectra of PVF_2 in the melt-quenched blends over the 920−820 cm^{-1} region.

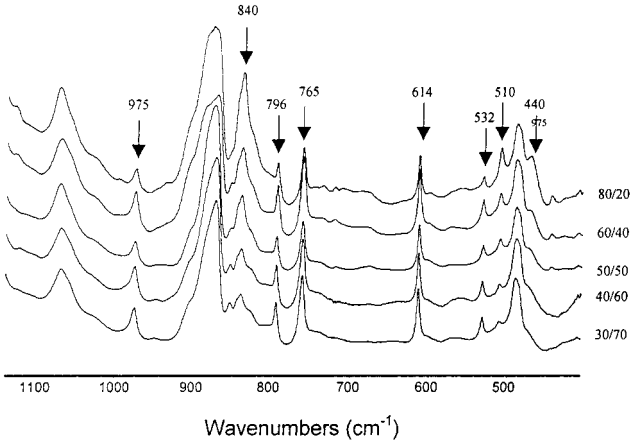

Figure 6. IR spectra of PVF_2 in the melt-quenched blends in 1100−440 cm^{-1} region after the subtraction of the nylon-11 absorbency.

polymorphic phases depending on crystallization condition such as temperature, solvent, and pressure. At least four crystal phases of PVF_2 have been found. Phase I has a planar (all-trans) zigzag chain conformation with the space group *Cm*2*m*. Phase II has a chain conformation approximately TGTG′ (trans−gauche−trans−gauche′) with the space group *P*2*cm*. Phase III has a chain conformation approximately TTTGTTTG′ with the space group *C*2*cm*.[21] Phase IV has the same chain conformation (TGTG′) as phase II, but with a polar space group *P*2*cn* and slight changes of the chain packing.[22] The vibrational spectra of the first three crystal phases are relatively well understood.[23−27] The IR spectra of phase I and II have been analyzed extensively.[26] The vibration bands at 532, 614, 765, 796, 854, 870, and 975 cm^{-1} correspond to phase II. The vibrational bands at 510, 840, and 877 cm^{-1} are assignable to phase I. The IR spectra of phase III are similar to those of phase I except for some extra bands, such as the weak band at 440 cm^{-1} and the strong band at 882 cm^{-1} which are characteristic of the phase III structure[27] (the 510 cm^{-1} band is characteristic of both phase I and phase III).

The above band intensity changes show that as nylon-11 concentration increased in the blends, some PVF_2 crystallized into phase I (polar) and phase III (polar) instead of phase II (nonpolar) as found in pure PVF_2 under similar melt-quench conditions. The relative amounts of phase I and III versus phase II could actually be determined from the relative intensity of the 510 cm^{-1} (phase I and III) and 530 cm^{-1} (phase II) bands,[28] CF_2 bending for the two phases, if we assume that these two bands have equivalent adsorption coefficients as was previously done.[29]

We conclude from the above IR results of nylon-11 and PVF_2 band changes in the powder blends that there are specific dipolar interactions between nylon-11 and PVF_2. Nylon-11 became more disordered as the PVF_2 concentration increased. Some portion of PVF_2 crystallized into polar phases instead of the nonpolar phase usually produced in pure PVF_2. This is consistent with the case of VF_2 copolymerized with small mole fractions of VF_3 (less than 20%), where the copolymers crystallize directly into polar phase I from the melt because the structural regularity of the VF_2 chains is disturbed by the presence of VF_3 units. The slight structural irregularity of PVF_2 makes it more favorable to develop the less stable polar phase I crystal than to develop the more stable nonpolar phase II crystal.

3. Crystal Phase Transformation and Electromechanical Properties of Uniaxially Oriented Blend Films. For ferroelectric polymers such as nylon-11 and PVF_2, we know that drawing significantly increases electroactive properties including piezoelectric properties.[30,31] It would therefore be of interest to investigate oriented blend films for piezoelectric applications. Because of the intermolecular interactions we examined above along with the change in glass transition temperature as well as crystal phase changes in both the nylon-11 and PVF_2 components in the melt-quenched blends, we expected that, during the drawing process, crystal phase transformations might be different from those of the pure polymers. We also expected that the electromechanical properties of these oriented blends might be different.

We measured the piezoelectric stress and strain coefficients, d_{31} and e_{31}, respectively, at 104 Hz at room temperature. Parts a and b of Figure 7 show d_{31} and e_{31}, respectively, of the blends at low nylon-11 concentrations. Both of d_{31} and e_{31} of the blends are larger than that of pure PVF_2 and nylon-11 at nylon-11 concentrations lower than 10%. The observed values obviously exceeded the additive rule of the composites.

Since piezoelectricity is a coupling of the mechanical and electrical properties of a material, we measured the mechanical and dielectric properties of the blends which are shown in Figure 8a,b. We see that the dielectric constants follow, approximately, a simple additive rule, but the Young's modulus shows higher values than the prediction of a simple additive rule in blends. This suggests that the enhancement of piezoelectric properties may come from a better crystal phase transformation of PVF_2 from phase II to phase I in the blends.

Figure 9 shows the IR spectra over the 1300−700 cm^{-1} region for drawn blends as well as drawn pure PVF_2 after the subtraction of the nylon-11 spectra, from

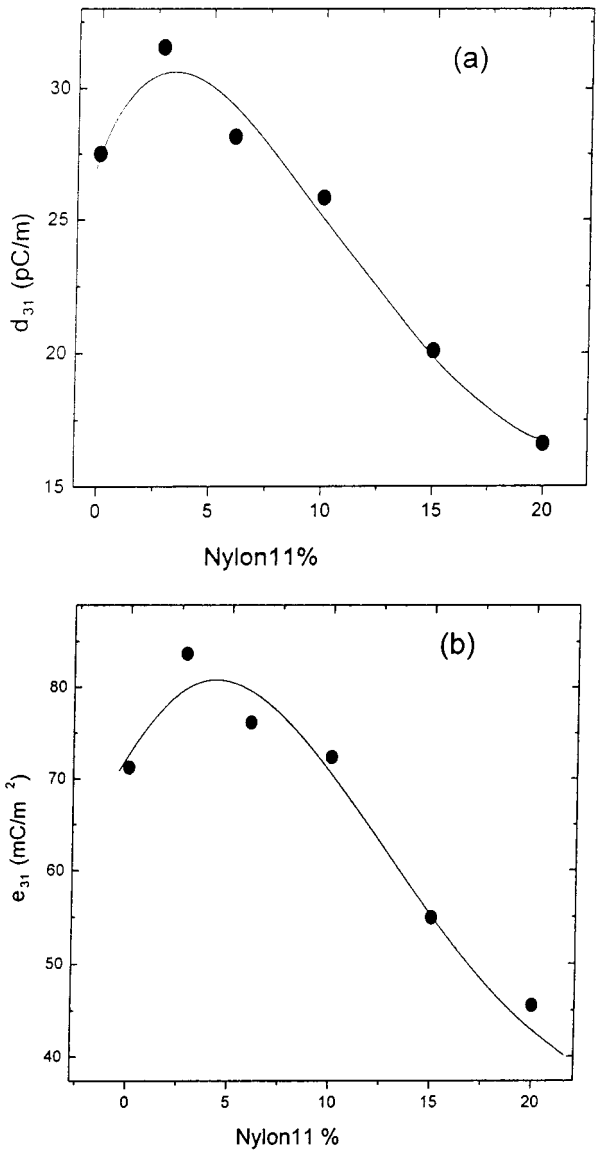

Figure 7. Piezoelectric stress and strain coefficients, (a) d_{31} and (b) e_{31}, of the blends at low nylon-11 concentrations.

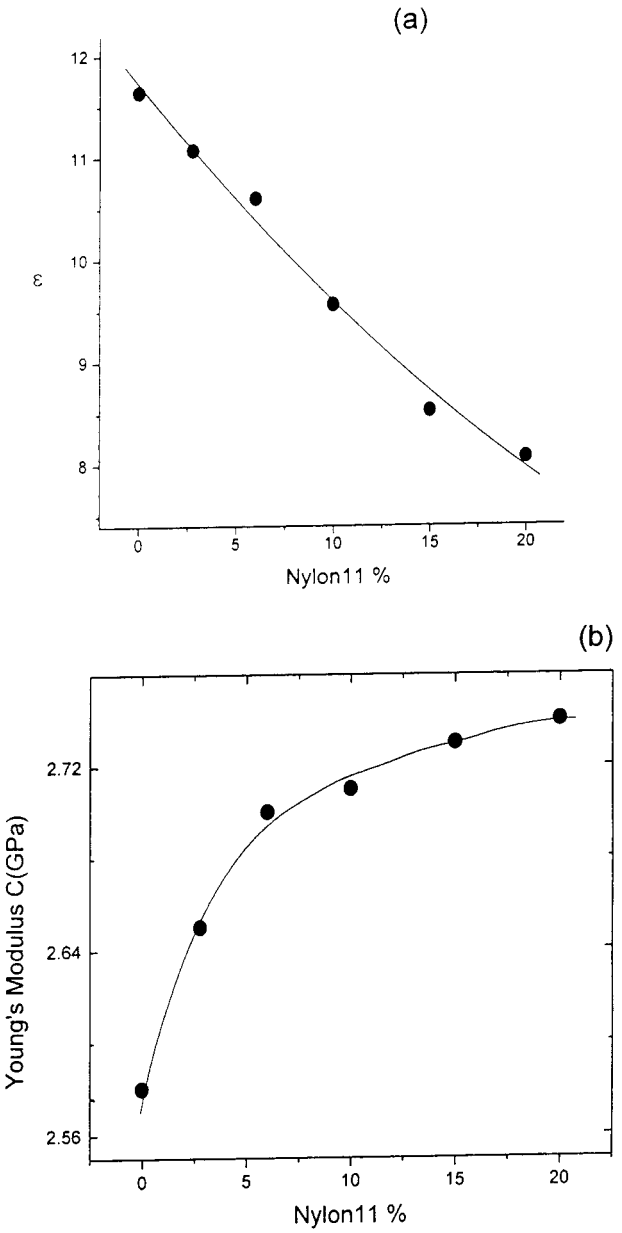

Figure 8. Mechanical and dielectric properties of the blends: (a) Young's modulus and (b) dielectric constant.

which we see that the drawing process transformed most of the phase II PVF_2 into phase I in both the pure and blend cases. However, some traces of the phase II characteristic bands, such as the 976 cm^{-1} band, were observed in drawn pure PVF_2 samples while there is no such band observed in the drawn blends.

We also used WAXD to study the crystal structure of the drawn blends. We observed a large peak at ~22°, which is the overlap of the 200/110 PVF_2 phase I and 200/020 nylon-11 crystal reflections. Figure 10 is a plot of the half-width of this peak versus composition of the blends. The peak half-width of the blends in the composition region 5/95 to 20/80 nylon-11/PVF_2 is smaller than that of either pure nylon-11 or pure PVF_2. This indicates that crystals developed in the blends after drawing are either bigger or more ordered than in the pure state.

To investigate the chain orientation of nylon-11 and PVF_2 in the blends, we measured the dichroic ratio of IR bands of nylon-11 (3300 cm^{-1}) and PVF_2 (870 cm^{-1}) versus blend composition as shown in Figure 11a,b. We measured 3−4 samples for each data point; the values agree within ±2.5%. The infrared dichroic ratio, R, is

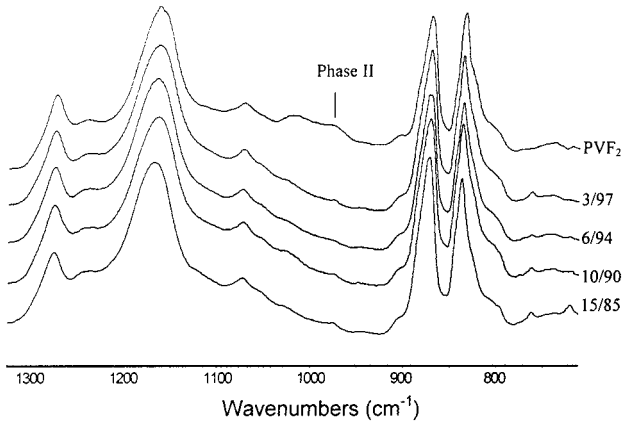

Figure 9. IR spectra of the drawn blends in 1300−700 cm^{-1} region after the subtraction of the nylon-11 absorbency.

equal to $A_{\parallel}/A_{\perp}$, where $A_{\parallel}$ and $A_{\perp}$ are the measured absorbency (intensity) of the electric vector parallel and perpendicular, respectively, to the drawing direction.

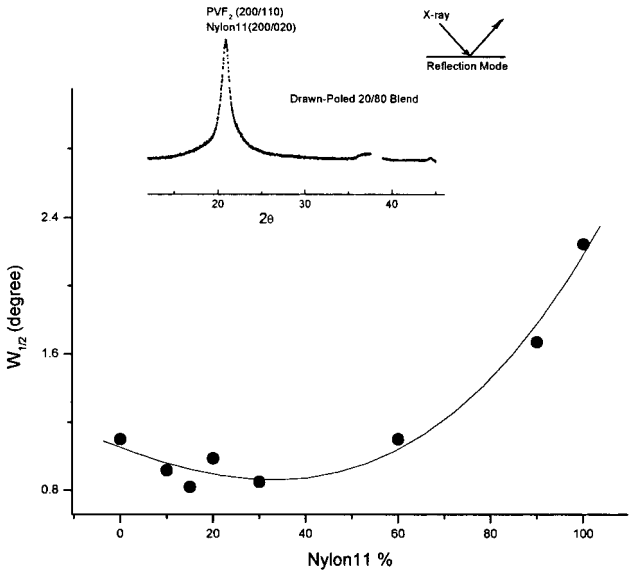

Figure 10. Half-width of X-ray diffraction peak at ~22° of the drawn blends versus composition.

There was little change in chain orientation of PVF_2 in the blends while nylon-11 chain orientation decreased. The chain orientation measured in polymer systems subjected to uniaxial drawing is generally composed of two principal factors. One is the orientation induced by the act of drawing. This is governed by the number of effective entanglements between chains. The other is related to the chain relaxation that inevitably occurs during the drawing process and which reduced orientation to some extent. It is well-known that the existence of specific interactions between chains in the system decreases or increases the rate of chain relaxation. The decrease of nylon-11 chain orientation in the blends may result from the enhanced chain relaxation rate due to specific interactions, which is shown as the decrease of the glass transition temperature of nylon-11 in the blends in section III.1.

From the above FTIR, IR dichroic ratio, and WAXD results, we concluded that the crystal phase transformation of PVF_2 from phase II to phase I was more complete in the blends than in pure PVF_2. The enhancement of piezoelectric properties we observed may also result from better PVF_2 crystals present in the blends. The phase transformation of PVF_2 phase II to phase I upon drawing is favored by blending with nylon-11, shown clearly by FTIR in the low nylon-11 concentration region. This is also confirmed by direct observations, in which the room-temperature drawing of the blends is much easier than that of pure PVF_2 film; i.e., the possibility of film breakage and necking is much lower, and the drawn blend films are visibly more uniform than the drawn pure PVF_2 films.

4. High-Temperature Stability of Piezoelectric Properties of the Blends. High-temperature stability is a significant issue in electroactive polymer applications. As stated in the Introduction, one of the motivations of this ferroelectric polymer blend study was to try to combine the high-temperature piezoelectric stability of nylons with the large room-temperature piezoelectric response of PVF_2.

We poled and then annealed drawn films of the blends as well as the homopolymers at 160 °C for 2 h under 10^{-3}psi vacuum. Parts a and b of Figure 12 show the temperature dependence of the piezoelectric coefficients,

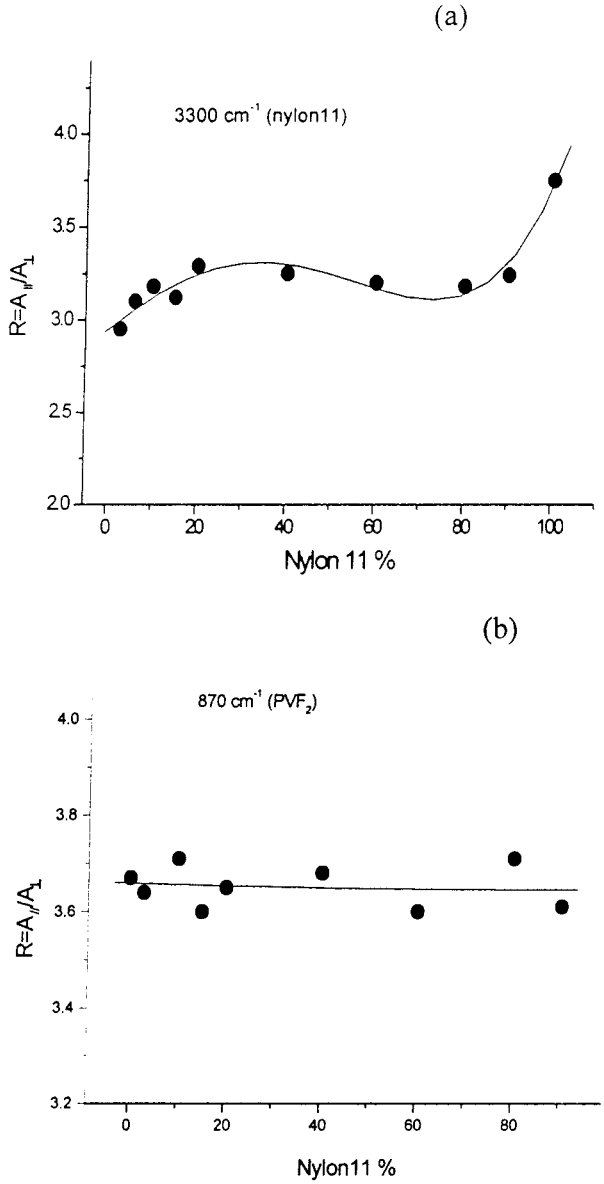

Figure 11. Dichroic ratio of IR bands versus composition of the drawn blends: (a) nylon-11, 3300 cm^{-1}; (b) PVF_2, 870 cm^{-1}.

d_{31} and e_{31}, respectively, for these poled-annealed films. In Figure 12a, we see that d_{31} of poled-annealed blends of 80/20, 50/50, and 20/80 nylon-11/PVF_2 are all larger than that of either component at high temperature, especially for the 20/80 and 80/20 blends. Figure 12b shows that the piezoelectric stress coefficient, e_{31}, of the 20/80 and 50/50 blends was also higher than those of the homopolymers, especially at the 20/80 composition. As previously known[13] and also shown in Figure 12a,b, nylon-11 exhibited little decay while PVF_2 showed a large decay in piezoelectric response after annealing. Figure 13a,b shows the composition dependence of d_{31} and e_{31} of blends at the highest measurement temperature, 160 °C. We measured 3−4 samples for each data point; the values agree within ±2.5%. It is seen that the blends at the 20/80 composition region exhibited high-temperature stability. The stabilized polarization of these blends may result from the better ordered phase I PVF_2 and the polar interactions between nylon-11 and PVF_2, where the stabilized nylon polar structure may "hold" much of the PVF_2 polarization in place at high temperatures.

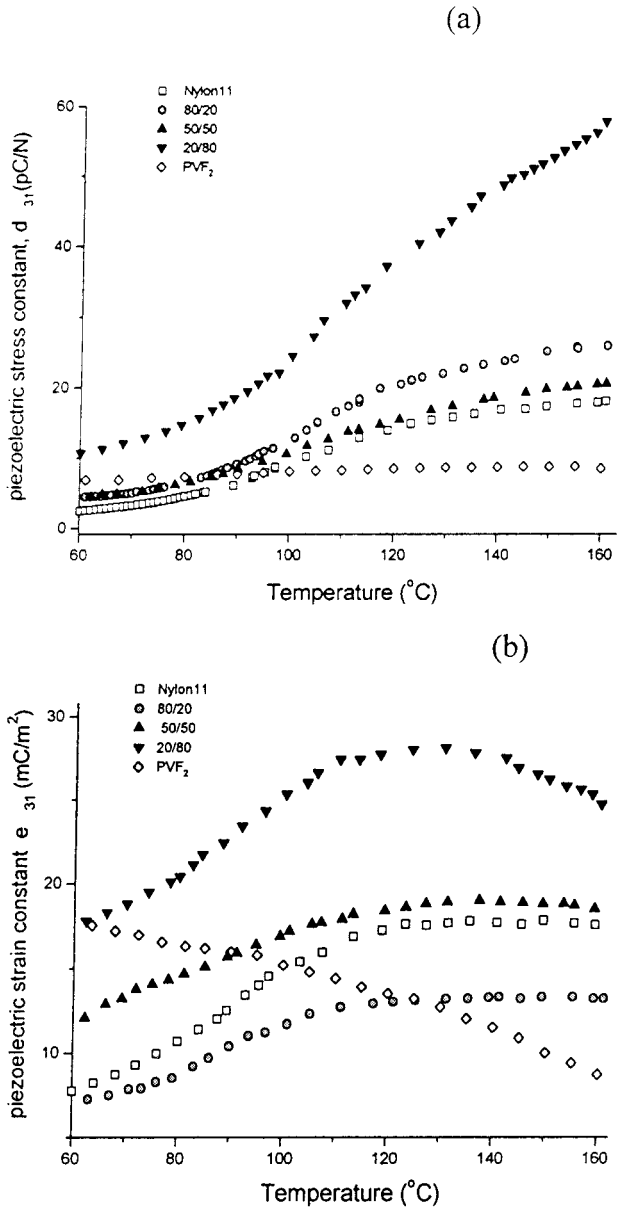

Figure 12. Temperature dependence of piezoelectric coefficients, (a) d_{31} and (b) e_{31}, for poled-annealed drawn blend films.

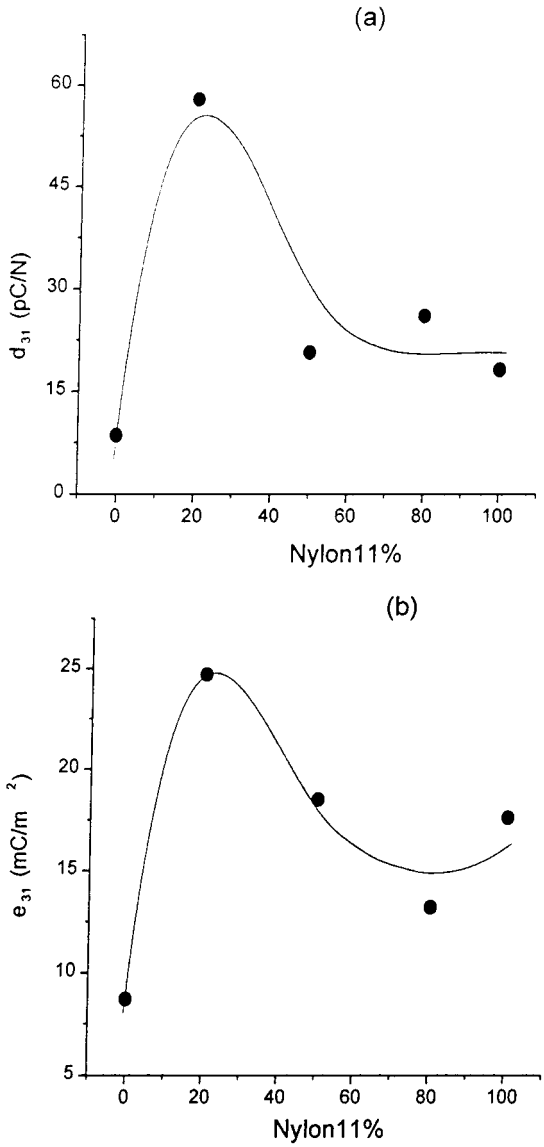

Figure 13. Composition dependence of d_{31} and e_{31} of the poled-annealed drawn blends at 160 °C.

IV. Conclusions

In this work, we investigated mechanically mixed powder blends of two ferroelectric polymers: nylon-11 and PVF_2. The interactions between these two polar semicrystalline polymers was evidenced by the observed decrease of the glass transition and melting point of nylon-11 with decreased nylon-11 concentration. FTIR measurements of melt-quenched blends showed that several characteristic bands of nylon-11 and PVF_2 changed with composition. The N−H stretching and amide I band of nylon-11, which characterize the secondary structure of nylons, shift to higher and lower wavenumbers, respectively, indicating that the nylon-11 H-bonded structure becomes more disordered in the blends. The PVF_2 skeletal band (870 cm^{-1}), which characterizes the chain conformation and crystal phase, shifts to lower wavenumber and becomes much broader in the blends. The band shifts also indicate that there are specific interactions between the polar amide groups (CONH) in nylon-11 and the polar CF_2 groups in PVF_2, which affect the crystallization behavior and phase transformations of both components in the blends. PVF_2 developed a large proportion of polar crystal phases in blends with high nylon-11 concentration compared to the nonpolar phase II developed in pure PVF_2 under similar melt-quench conditions. During the uniaxial drawing process of these melt-quenched samples, the phase transformation of PVF_2 from nonpolar phase II to polar phase I was more complete, and the resulting phase I was more ordered in the blends than in pure PVF_2 as shown by FTIR and WAXD, although the average chain orientation of the components changed little as shown by the dichroic ratio. We found that this led to an enhancement (30% increase) in piezoelectric properties of the blends at low nylon-11 concentration. In addition, we achieved significant high-temperature piezoelectric stability up to 160 °C in the blends, which is crucial to many applications of electroactive polymers. The improved thermal stability of the polarization in the blends may result from a more ordered PVF_2 phase I crystal structure and the stronger dipolar intermolecular interactions between nylon-11 and PVF_2 compared to those of the homopolymer. Annealing makes the nylon-11 piezoelectric response stable to the melt

temperature.[15] This may "hold" much of the PVF_2 polarization in place at high temperature.

Acknowledgment. We thank Mark Paczkow at Bell Labs for useful discussions and the use of his FTIR spectrometer. This work was supported by ONR, CAFT, and NSF.

References and Notes

(1) Nalwa, H. S.; et al. *Ferroelectric Polymers: Chemistry, Physics and Applications;* Marcel Dekker: New York, 1995.
(2) Kepler, R. G. In *Ferroelectric Polymers: Chemistry, Physics and Applications*; Nalwa, H. S., et al., Eds.; Marcel Dekker: New York, 1995; Chapter 3.
(3) Scheinbeim, J. I.; Newman, B. A. *Trends Polym. (TRIP)* **1993**, *1*, 394.
(4) Dondos, A.; Pierri, E. *Polym. Bull.* **1986**, *16*, 567.
(5) Bernstein, R. E.; Paul, D. R.; Barlow, J. W. *Polym. Eng. Sci.* **1978**, *18*, 683.
(6) Jungnickel, B. J. In *Ferroelectric Polymers: Chemistry, Physics, and Applications*; Nalwa, H. S., et al., Eds.; Marcel Dekker: New York, 1995; Chapter 4.
(7) Galin, M. *Makromol. Chem. Rapid Commun.* **1984**, *5*, 119.
(8) Liu, Z.; Marechal, P.; Jerome, R. *Polymer* **1997**, *38*, 5149.
(9) Demont, P.; Fourmand, L.; Chatain, D.; Lacabane, C. *Adv. Chem. Ser.* **1990**, *227*, 191.
(10) Zhang, X.; Shimoda, M.; Toyoda, A. *Polymer* **1994**, *32*, 4280.
(11) Coleman, M. M.; Zarian, J. *J. Polym. Sci., Phys Ed.* **1979**, *17*, 837.
(12) Bottino, A.; Capannelli, G.; Munari, S.; Turturro, A. *J. Polym. Sci., Polym. Phys. Ed.* **1988**, *26*, 785.
(13) *CRC Handbook of Polymer-Liquid Interaction Parameters and Solubility Parameters;* CRC Press: Boca Raton, FL, 1986; pp 39−40.
(14) Gao, Q.; Scheinbeim, J. I.; Newman, B. A. *J. Polym. Sci., Polym. Phys. Ed.* **1999**, *37*, 3217.
(15) Takase, Y.; Lee, J. W.; Scheinbeim, J. I.; Newman, B. A. *Macromolecules* **1991**, *24*, 4**,** 6644.
(16) Penning, J. P.; St. John Manley, R. *Macromolecules* **1996**, *29*, 77.
(17) Nishi, T.; Wang, T. T. *Macromolecules* **1975**, *8*, 909.
(18) Byler, D.; Susi, H. *Biopolymers* **1986**, *25*, 469.
(19) Skrovanek, D. J.; Painter, P. C.; Coleman, M. M. *Macromolecules* **1986**, *19*, 699.
(20) Kinoshita, Y. *Makroml. Chem.* **1959**, *33*, 1.
(21) Weinhold, S.; Litt, M. H.; Lando, J. B. *Macromolecules* **1980**, *13*, 1178.
(22) Bachmann, M.; Gorgon, W. L.; Weinhold, S.; Lando, J. B. *J. Appl. Phys.* **1980**, *51*, 5095.
(23) Prest, W. M., Jr.; Lin, D. J. *J. Appl. Phys.* **1975**, *46*, 4136.
(24) Kobayashi, M.; Tashiro, K.; Tadokoro, H. *Macromolecules* **1975**, *8*, 158.
(25) Cortill, G.; Curro, G. *J. Polym. Sci., Polym. Phys. Ed.* **1967**, *12*, 2216.
(26) Boerio, F. J.; Koenig, J. L. *J. Polym. Sci., Part A2* **1974**, *9*, 1517.
(27) Bachmann, M.; Gorgon, W. L.; Koenig, J. L.; Lando, J. B. *J. Appl. Phys.* **1979**, *50*, 6106.
(28) Yang, D.; Thomas, E. L. *J. Mater. Sci., Lett.* **1987**, *6*, 593.
(29) Hsu, S. L.; Lu, F. J.; Waldman, D. A.; Muthukumar, M. *Macromolecules* **1985**, *18*, 2583.
(30) Wu, S. L.; Scheinbeim, J. I.; Newman, B. A. *J. Polym. Sci., Polym. Phys.* **1999**, *37*, 2737.
(31) Shuford, R. J.; Wilde, A. F.; Ricca, J. J.; Thomas, G. R. *Polym. Eng. Sci.* **1976**, *16*, 25.

MA000111I